Dental Materials Journal 2019; 38(4): 534–539

Size effect of nano-hydroxyapatite on proliferation of odontoblast-like MDPC-23 cells

Na LI[1]*, Gang WU[2], Hua YAO[3], Ruikang TANG[4], Xinhua GU[3] and Chengwei TU[2,5]*

[1] *Department of Oral Medicine, School and Hospital of Stomatology, Wenzhou Medical University, Wenzhou, Zhejiang, 325000, China*
[2] *Department of Oral Implantology and Prosthetic Dentistry, Academic Center for Dentistry Amsterdam (ACTA), University of Amsterdam, Gustav Mahlerlaan 3004, 1081LA Amsterdam, Nord-Holland, The Netherlands*
[3] *Department of Stomatology, the First Affiliated Hospital, College of Medicine, Zhejiang University, Hangzhou, 310003, China*
[4] *Department of Chemistry, Center for Biomaterials and Biopathways, Zhejiang University, Hangzhou, 310027, China*
[5] *Department of Stomatology, the First Affiliated Hospital, Wenzhou Medical University, Wenzhou, Zhejiang, 325006, China*
Corresponding author, Chengwei TU; E-mail: 175193674@qq.com, Xinhua GU; E-mail: guxh@zje.edu.cn

Nano-hydroxyapatite (nano-HAP) is supposed to be a promising candidate for apatite substitute in hard tissue engineering. We aimed to investigate the effect of nano-HAP particles on the proliferation of odontoblast-like MDPC-23 cells compared with conventional hydroxyapatite (c-HAP). HAP in diameter of ~20 nm (np20), ~70 nm (np70) and ~200 nm (c-HAP) were synthesized and characterized by Fourier transform infrared spectroscopy (FTIR), X-ray diffraction (XRD), transmission electron microscopy (TEM) and field emission scanning electron microscopy (FESEM). Inverted microscope and MTT assay were used to detect the morphology and proliferation rate of MDPC-23 cells; TEM was used to reveal the internalization of HAP. We found that nano-HAP (np20 and np70), especially np20 expressed obvious growth-promoting effect on MDPC-23 cells compared with c-HAP, which caused the most vacuole in MDPC-23 cells. These results suggest that nano-HAP may be an optimal choice of apatite substitute for MDPC-23 cells on the aspect of cell proliferation.

Keywords: Nano-hydroxyapatite, Odontoblast-like cell, MDPC-23, Cell proliferation, MTT assay

INTRODUCTION

Caries, also known as dental decay or cavities, is a breakdown of teeth due to acids made by bacteria[1]. In 2016, approximately 2.44 billion people have dental caries in their permanent teeth worldwidely, which ranked the first of the ten causes with the greatest prevalence for the global burden of disease[2]. Once the caries is removed, restorative materials are needed to repair the defect of the teeth. By far, composite resin bonding technique has become the main treatment for dental decay. However, the limited durability of resin-dentin bonds severely compromises the lifetime of adhesive-related restorations[3]. Regenerated dentin is considered to be the ideal material for dentin restoration. Hence, dentin regeneration has been a hot research area recently, in which biomimetic mineralization and remineralization are the main strategies[4,5].

Hydroxyapatite (HAP) is a naturally occurring mineral form of calcium apatite with the formula $Ca_{10}(PO_4)_6(OH)_2$, which composed up to 70% by weight of human bone and tooth[6]. It has been widely used as a filler to replace amputated bone or as a coating to promote bone ingrowth into prosthetic implants in many surgical fields such as the reconstructive surgeries[7-9] and dental implantology[10]. It is also being used to repair early lesions in tooth enamel[11]. In spite of attractive biological properties, hydroxylapatite has some drawbacks, such as low bioresorption rate *in vivo*, poor stimulating effect on the growth of new bone tissues, low crack resistance and small fatigue durability in the physiological environment. The nanocrystallization of hydroxylapatite opens up the opportunities for advanced applications in fields of biomedical materials and have aroused intensive interest in the last decade[12].

Nano-hydroxyapatite (nano-HAP), which shares the same inorganic building blocks of tooth and bone may be a promising candidate for an apatite substitute in hard tissue engineering. The previous studies have demonstrated that 25–50 nm apatite particles play an important role in bio-mineral formation[13]. It is suggested that tens of hundreds of nano-sized apatite particles packed densely into woven collagen in terms of remarkable physical and chemical features, such as unique mechanical strength, improved biocompatibility, and good bioactivity[14-17]. Therefore, great efforts have been made to study their synthesis and intricate properties[18-22]. The study of Cai *et al.* showed that the nano-HAP, especially for 20 nm sized particles, showed improved cytophilicity for the bone marrow mesenchymal stem cells (MSCs) as compared with conventional HAP[23]. Yang *et al.*[24] found that the incorporation of nano-HAP in nanofibers indeed enhanced dental pulp stem cells (DPSCs) differentiation towards an odontoblast-like phenotype *in vitro* and *in vivo*. However, the effect of the size of nano-HAP on odontoblast-like cells, especially

*Authors who contributed equally to this work.
Color figures can be viewed in the online issue, which is available at J-STAGE.
Received May 18, 2018: Accepted Oct 9, 2018
doi:10.4012/dmj.2018-155 JOI JST.JSTAGE/dmj/2018-155

the MDPC-23 cells still remain unknown.

In this study, HAP with diameters of ~20, ~70 and ~200 nm were synthesized and characterized, and the effect of these HAP particles on the proliferation of odontoblast-like cell line (MDPC-23 cells) were evaluated *in vitro*.

MATERIALS AND METHODS

Preparation and characterization of HAP

The chemicals were analysis-grade and purchased from Sinopharm Chemical Reagent (Shanghai, China). The size-controlled nano-HAP particles were prepared as previous described[23]. Hexadecyl(cetyl) trimethyl ammonium bromide (CTAB) was used to regulate the size of nano-HAP particles according to the theory of critical micelle concentration (CMC)[25]. Briefly, the size-controlled nano-HAP particles were synthesized by dropping 5.0 mM $CaCl_2$ (60 mL) to 1.25 mM Na_2HPO_4 solutions (240 mL) in the presence of CTAB (6.0×10^{-4} or 12.0×10^{-4} M) in magnetically stirred vessels at 20°C. The pH of the solutions was maintained at 10.0±0.5 by the addition of 0.1 M ammonia. The suspension was then stirred at 20°C for another 24 h to allow the completion of particle formation. The precipitate was filtered (0.22 μm Millpore filter) and washed with distilled water. After drying in a vacuum at 40°C, solids were washed with ethanol to dissolve residual CTAB molecules and separated from the CTAB by five 10 min cycles of centrifugation at 1,800 g. The calcium phosphate particles in the precipitate were then dried in a vacuum at room temperature. Convetional HAP particles (c-HAP) were prepared regularly as described by Nancollas and Mohan[26].

All the obtained particles were characterized by X-ray diffraction (XRD; Rigaku D/max-2550 pc, Tokyo, Japan) with Cu Ka radiation. Field emission scanning electron microscopy (FESEM; Hitachi4700, Tokyo, Japan) and transmission electron microscopy (TEM; JEM-200CX, Rigaku, operated at 160 KV) were used to examine the morphologies of the solids. Data were analyzed based on six replicated tests.

Cell culture

The odontoblast-like cell line which derived from the mouse dental papilla (MDPC-23, a generous gift from Prof. Hanks CT, School of Dentistry, University of Michigan, MI, USA) was used in this study. Cells were seeded at $3.0\times10^5 cm^{-2}$ in Dulbecco's Modified Eagle's Medium (DMEM; Gibco, Grand Island, NY, USA) containing 10% fetal bovine serum (FBS; Gibco) and maintained in a humidified atmosphere with 5% CO_2 at 37°C. The medium was renewed three times a week. The MDPC-23 cells initially grew to 70–90% confluence in culture flasks and were re-suspended at $1.0\times10^5 cm^{-2}$ after harvesting with 0.02% EDTA and 0.25% trypsin and kept cultivating for next usage.

Morphological observation by inverted microscope

MDPC-23 cells were seeded into 24-well microtiter plate (with a density 3×10^4 cells/well) and were incubated for 24 h at 37°C and 5% CO_2. Then the cells were treated with HAP suspension containing different-sized particles (~20, ~70 and ~200 nm) with the same concentration of 40 ng/mL and medium only (control), then incubated for 1, 3 and 5 days. The cellular morphological changes of the treated and untreated cells were observed under a Leica DM IRB (Leica Microsystems, Wetzlar, Germany) inverted microscope.

MTT assay of cell proliferation

MTT [3-(4,5-dimethyl-2-thyazolyl)-2,5-diphenyl-2H-tetrazolium-bromidecolorimetric] which can be converted by living cells into a blue/purple formazan product reflects cell proliferation *in vitro* since the intensity of the color is directly related to the number of viable cells. So, we used MTT assay to measure the size effect of HAP particles on cell proliferation of MDPC-23. Well-growing MDPC-23 were collected and seeded in 96-well plates (Corning Costar) at 5×10^3 per well. Cells were cultured with 40 ng/mL HAP suspension containing particles of different sizes (~20, ~70 and ~200 nm) and medium only (control). Six duplicate wells were set up in each sample. During incubated at 37°C, 5% CO_2 for 5 days, viable cell number was detected by MTT at the first, third and fifth day randomly. Cells were incubated at 37°C for 4 h after the addition of 50 μL of MTT to each well and then the MTT medium was discarded and 0.5 mL dimethylsulfoxide (DMSO) of 37°C was added. After solubilization of the blue formazan product with DMSO, we used a microplate reader (BioTek EL800, Winooski, VT, USA) to detect the absorbance at 490 nm which was expressed by optical density value (OD value). The background OD value of wells containing no cell was subtracted from the absorbance for all experimental samples. Measurements from six samples were used to determine the mean value of each group.

TEM observation of the uptake activity

TEM was used to visualize cellular uptake of HAP particles. Briefly, MDPC-23 cells were seeded in six-well plates and cultured with 40 ng/mL HAPs for 24 h. After incubation, MDPC-23 cells were detached by 0.25% trypsin-EDTA, then fixed with 2.5% glutaraldehyde. After treatment with 1% osmium tetroxide, the samples were dehydrated with a series of alcohols and infiltrated with epoxy resin. The resin sample block was trimmed, thin-sectioned and collected on formvar-coated copper grids. Thin sections were stained in uranyl acetate and lead citrate for examination by TEM (JEM-200CX).

Statistical analysis

All quantitative experiments were performed three times separately. Data was presented as mean values±SD and analyzed using SPSS 19.0 software. The one-way analysis of variance (ANOVA) was used for statistical analysis. $p<0.05$ was considered statistically significant.

RESULTS

Characteristics of synthesized nano-HAP and c-HAP

FESEM showed that the structure of particle surface was uniform (Fig. 1-A). TEM showed that the particles of nano-HAP were sphere-like with diameters of ~20 and ~70 nm and the particles with approximate diameters of 200 nm (c-HAP) were rod-like (Fig. 1-B).

The fourier transform infrared spectroscopy (FTIR) spectra (Fig. 1-C) of three synthesized HAPs featured phosphate absorption bands. The triply degenerated asymmetric stretching and bending vibrations of PO_4^{3-} were at 1,030 and 570 cm^{-1}. The peaks of CO_3^{2-} (1,420 and 875 cm^{-1}) implied that some carbonate ions were incorporated into np20, np70 and c-HAP. The incorporation of carbonate is a universal phenomenon during the formation of biological apatites. In these experiments, the carbonate substitution may come from CO_2 in the atmosphere, dissolved in the solutions which were used for the preparation of the nano-HAP particles. The peaks at 3,435 and 1,640 cm^{-1} related to the remaining water. No peaks of CTAB (2,800–3,000 cm^{-1}) were detected in either sample.

XRD patterns (Fig. 1-D) of three particles with different sizes indicated that only the HAP phase without any other phases was found, and all the diffraction peaks could be assigned according to the standard HAP (JCPDS09-0432).

MTT assay and morphology of MDPC-23 under inverted microscope

As shown in Fig. 2-A, the MDPC-23 cells incubated with np20, np70 and c-HAP suspension proliferated with increasing culturing time (up to 5 days), which was indicated by the OD value of MTT assay. Furthermore, viable cell number was significantly higher in np20 compared to c-HAP after 3 and 5 days of incubation, though there was no significant difference between each two groups after 1 day of incubation. Moreover, the OD value of MDPC-23 cells in np70 became higher than that of c-HAP only after 5 days of incubation and was significantly lower than that of np20 after 3 and 5 days of incubation, but the gap between np20 and np70 shrunk with the prolongation of culture time. These

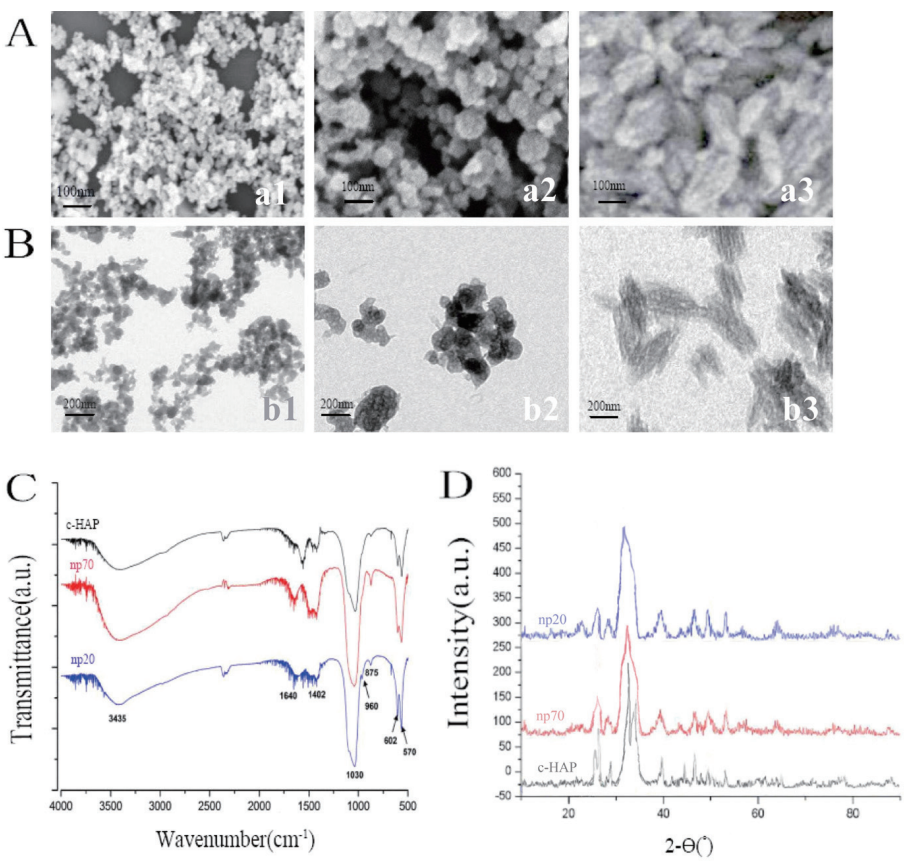

Fig. 1 Characteristics of particles of synthesized hydroxyapatite in diameter of ~20 nm (np20), ~70 nm (np70) and coventional HAP (c-HAP).
(A) FESEM images of np20 (a1), np70 (a2) and c-HAP (a3); (B) TEM images of np20 (b1), np70 (b2) and c-HAP (b3); (C) FTIR patterns of np20, np70 and c-HAP; (D) XRD patterns of np20, np70 and c-HAP.

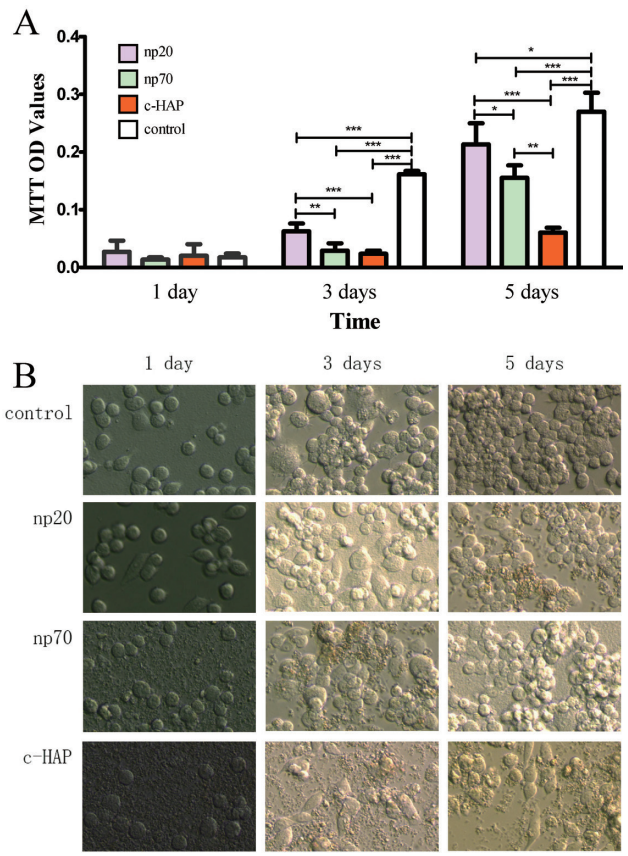

Fig. 2 (A) Columns of MTT assays of nano- hydroxyapatite in diameter of ~20 nm (np20) or ~70 nm (np70), coventional HAP (c-HAP) and only cell culture medium (control) on numbers of viable MDPC-23, *p<0.05, **p<0.01, ***p<0.001. (B) Inverted microscopic photographs of MDPC-23 cells co-cultured with cell culture medium only (control), nano-HAP in diameter of ~20 nm (np20) or ~70 nm (np70) and coventional HAP (c-HAP) for 1, 3 and 5 days.

are consistent with the results of inverted microscope observation, which showed that the cell coverage of np20 was higher than that of np70 and c-HAP after 5 days of culture. Though the viable cell number of the control group was the most among all groups after incubation of 3 and 5 days, there was no apparent morphological differences between each two groups (Fig. 2-B).

Uptake of HAP by MDPC-23

Through comprehensive investigation of TEM on the cellular uptake of HAP, we found that HAP was either located in the cytoplasmic vesicles or clustered in the cytoplasm of MDPC-23 cells, and did not enter the nucleus. As the particle diameter increases, HAP caused more vacuoles in the cytoplasm of cells (Fig. 3).

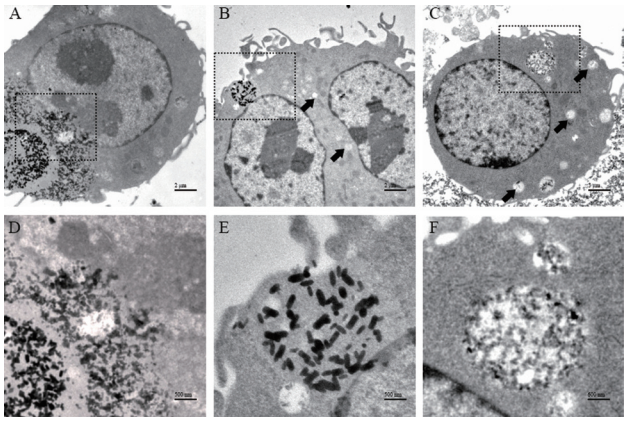

Fig. 3 TEM photographs of internalization and intracellular distribution of HAP in MDPC-23 exposed for 24 h.
Notes: MDPC-23 treated with np20 (A and D), np70 (B and E) and c-HAP (C, F). Overall cell morphology (A, B and C), scale bar: 2 μm. Higher magnification of cells in dotted boxed areas (D, E and F), scale bar: 500–600 nm. The black arrow indicates vacuoles in the cytoplasm.

DISCUSSION

The microstructure of nano-HAP is similar to that of natural bone and tooth[27,28], conferring itself the special biological characteristics, such as non-immunogenicity, non-inflammatory behavior, good biocompatibility, high osteoconductivity and osteoinductivity[23,29-31]. It has been identified by many studies that nano-HAP of various forms has excellent compatibility with human osteoblast, and can promote its adhesion and proliferation[31-37]. What is more, 20 nm-sized nano-HAP (np20) has been reported to facilitate the growth of osteocyte more remarkably compared to nano-HAP of other size[38]. However, studies of effect of nano-HAP particles on odontoblast or odotablast-like cells are very rare.

The bioactivity of odontoblast is almost as same as that of osteoblast, which can produce hard tissues of human organ by biological mineralization. Our results suggest that np20 and np70 have obvious growth-promoting effect on MDPC-23 compared with conventional HAP. What is more, np20 was the most effective of the three different-sized HAP particles. The results agree with the finding of Shi *et al.* about the effect of nano-HAP on MG-63 cells[38]. Referring to other studies, we assume that nano-HAPs provide a higher surface per HAP volum for cell growth than c-HAP, which may result in increased cellular adherence and proliferation[39,40]. Additionally, smaller HAP nanoparticles could enter into cells more easily and stimulate cell growth[41]. So, advanced study should be carried out to testify whether nano-HAP promotes cell proliferation of MDPC-23 cells *via* the mechanism mensioned above.

Besides particle size, the crystallinity and the

morphology of HAP particles also affect cell proliferation. Our present study demonstrated that nano-HAP appeared less crystalline than the c-HAP and induced more proliferation of MDPC-23 cells, agreeing with previous studies which provided evidence that the crystallinity of calcium phosphate affects the behavior of cultured osteogenic cells[42]. Moreover, the morphology plays another important role for estimating the biological effect of calcium phosphate particles. In our study, rod-like HAP (c-HAP) and sphere-like HAP (np20 and np70) were obtained by controlling the CTAB concentration[43], and the cell experiment showed that HAP with spherical nanocrystals showed more favorable properties than rod-like HAP for odontoblast-like cells.

Considering the importance of internalization and subcellular localization on biological results, we studied the uptake and biological distribution of HAP. It was observed in TEM that HAP of three different sizes all could enter into MDPC-23 within 24 h and existed in the form of phagocytic vacuole, and the procedure might be relative to celluar reaction. MDPC-23 co-cultivated with c-HAP had largest quantity of vacuole. Some previous studies have shown that only the HAP in the nuclei may cause cytotoxicity, while the HAP in the cytoplasm will only cause slight change of the morphology and structure of the cell membrane and generate negligible inhibition[44,45]. However, our research results show that although np20 showed higher uptake, but np70 and c-HAP has a more significant inhibitory effect on the proliferation of MDPC-23, this means that the cell uptake is not the only factor in determining the biological results, other factors, such as shape, size and crystallinity might involve the biological interactions.

Cytotoxicity was another necessary parameter to evaluate the biological properties of HAP particles. In our experiment, MTT assay was used to reflect the number of vital cells in different groups, and the results showed that compared with the blank control group, the number of vital cells in the np20, np70 and c-HAP groups showed a downward trend at the same observation point, especially the np70 and c-HAP groups. Under an inverted microscope, np70 and c-HAP groups showed a significant decrease in cell density and a decrease in cell contact at the late stage of culture. More vacuoles were found in the cytoplasm of the np70 and c-HAP groups in the TEM test. These results suggest that larger nanoparticles and hydroxyapatite are toxic to cells. The specific mechanism of cytotoxicity is to be further investigated and validated by subsequent tests of apoptosis, which is assumed to be responsible for the toxic effect of HAP particles[46].

CONCLUSIONS

In this preliminary study, we synthesized HAP particles of different sizes and evaluated their effect on cell proliferation of odontoblast-like cells. It was demonstrated that cell proliferation are related to the size of the HAP particles inversely, which means np20 was the most effective at promoting cell growth of MDPC-23. According to our present study, nano-HAP may be an optimal choice of apatite substitute for MDPC-23 cells. Further studies, such as mineralization of HAP nanoparticle on MDPC-23 and *in vivo* experiments should be carried out before clinical application.

ACKNOWLEDGMENTS

Authors would like to thank Prof. Hanks CT for his present of MDPC-23 cell line, and also thank the support funding from the program of basic public welfare research of Zhejiang Province (NO. LGF18H140001) and the Natural Science program of Zhejiang Province (NO. LY16H140001).

REFERENCES

1) Silk H. Diseases of the mouth. Prim Care 2014; 41: 75-90.
2) GBD 2016 disease and injury incidence and prevalence collaborators. Disease, injury, and prevalence, global, regional, and national incidence, prevalence, and years lived with disability for 328 diseases and injuries for 195 countries, 1990-2016: a systematic analysis for the global burden of disease study 2016. Lancet 2017; 390: 1211-1259.
3) Liu Y, Tjäderhane L, Breschi L, Mazzoni A, Li N, Mao J, *et al.* Limitations in bonding to dentin and experimental strategies to prevent bond degradation. J Dent Res 2011; 90: 953-968.
4) Wu XT, Mei ML, Li QL, Cao CY, Chen JL, Xia R, *et al.* A direct electric field-aided biomimetic mineralization system for inducing the remineralization of dentin collagen matrix. Materials (Basel) 2015; 8: 7889-7899.
5) Han M, Li QL, Cao Y, Fang H, Xia R, Zhang ZH. In vivo remineralization of dentin using an agarose hydrogel biomimetic mineralization system. Sci Rep 2017; 7: 41955.
6) Contributors. Hydroxylapatite. 2018; Available from: https://en.wikipedia.org/w/index.php?title=Hydroxylapatite&oldid=830348791.
7) Matsumine A, Kusuzaki K, Matsubara T, Okamura A, Okuyama N, Miyazaki S, *et al.* Calcium phosphate cement in musculoskeletal tumor surgery. J Surg Oncol 2006; 93: 212-220.
8) Dorozhkin SV, Epple M. Biological and medical significance of calcium phosphates. Angew Chem Int Ed Engl 2002; 41: 3130-3146.
9) Hench LL. Bioceramics. J Am Ceram Soc 1998; 81: 1705-1728.
10) John L, Janeta M, Szafert S. Designing of macroporous magnetic bioscaffold based on functionalized methacrylate network covered by hydroxyapatites and doped with nano-$MgFe_2O_4$ for potential cancer hyperthermia therapy. Mater Sci Eng C Mater Biol Appl 2017; 78: 901-911.
11) Brunton PA, Davies RP, Burke JL, Smith A, Aggeli A, Brookes SJ, *et al.* Treatment of early caries lesions using biomimetic self-assembling peptides: a clinical safety trial. Br Dent J 2013; 215: E6.
12) Lu YP, Chen YM, Li ST, Wang JH. Surface nanocrystallization of hydroxyapatite coating. Acta Biomater 2008; 4: 1865-1872.
13) Olszta MJ, Cheng X, Jee SS, Kumar R, Kim YY, Kaufman MJ, *et al.* Bone structure and formation: A new perspective. Mater Sci Eng R Rep 2007; 58: 77-116.
14) Hassenkam T, Fantner GE, Cutroni JA, Weaver JC, Morse DE, Hansma PK. High-resolution AFM imaging of intact and fractured trabecular bone. Bone 2004; 35: 4-10.
15) Huang J, Lin YW, Fu XW, Best SM, Brooks RA, Rushton N, *et al.* Development of nano-sized hydroxyapatite reinforced composites for tissue engineering scaffolds. J Mater Sci Mater Med 2007; 18: 2151-2157.

16) Chen F, Lam WM, Lin CJ, Qiu GX, Wu ZH, Luk KD, *et al.* Biocompatibility of electrophoretical deposition of nanostructured hydroxyapatite coating on roughen titanium surface: In vitro evaluation using mesenchymal stem cells. J Biomed Mater Res B Appl Biomater 2007; 82: 183-191.
17) Lewandrowski KU, Bondre SP, Wise DL, Trantolo DJ. Enhanced bioactivity of a poly(propylene fumarate) bone graft substitute by augmentation with nano-hydroxyapatite. Biomed Mater Eng 2003; 13: 115-124.
18) Olton D, Li J, Wilson ME, Rogers T, Close J, Huang L, *et al.* Nanostructured calcium phosphates (NanoCaPs) for non-viral gene delivery: Influence of the synthesis parameters on transfection efficiency. Biomaterials 2007; 28: 1267-1279.
19) Phillips MJ, Darr JA, Luklinska ZB, Rehman I. Synthesis and characterization of nano-biomaterials with potential osteological applications. J Mater Sci Mater Med 2003; 14: 875-882.
20) Sheikh FA, Barakat NA, Kanjwal MA, Nirmala R, Lee JH, Kim H, *et al.* Electrospun titanium dioxide nanofibers containing hydroxyapatite and silver nanoparticles as future implant materials. J Mater Sci Mater Med 2010; 21: 2551-2559.
21) Roy M, Bandyopadhyay A, Bose S. Induction plasma sprayed nano hydroxyapatite coatings on titanium for orthopaedic and dental implants. Surf Coat Technol 2011; 205: 2785-2792.
22) Sheikh FA, Barakat NA, Kanjwal MA, Park SJ, Park DK, Kim HY. Synthesis of poly(vinyl alcohol) (PVA) nanofibers incorporating hydroxyapatite nanoparticles as future implant materials. Macromol Res 2010; 18: 59-66.
23) Cai Y, Liu Y, Yan W, Hu Q, Tao J, Zhang M, *et al.* Role of hydroxyapatite nanoparticle size in bone cell proliferation. J Mater Chem 2007; 17: 3780-3787.
24) Yang X, Yang F, Walboomers XF, Bian Z, Fan M, Jansen JA. The performance of dental pulp stem cells on nanofibrous PCL/gelatin/nHA scaffolds. J Biomed Mater Res A 2010; 93: 247-257.
25) Moulik SP, Haque Mde, Jana P, Das AR. Micellar properties of cationic surfactants in pure and mixed states. J Physic Chem 1996; 100: 701-708.
26) Nancollas GH, Mohan MS. The growth of hydroxyapatite crystals. Arch Oral Biol 1970; 15: 731-745.
27) Webster TJ, Ergun C, Doremus RH, Siegel RW, Bizios R. Enhanced osteoclast-like cell functions on nanophase ceramics. Biomaterials 2001; 22: 1327-1333.
28) Hench LL, Polak JM. Third-generation biomedical materials. Science 2002; 295: 1014-1017.
29) Vallet-Regi M, Gonzalez-Calbet JM. Calcium phosphates as substitution of bone tissues. Prog Solid State Chem 2004; 32: 1-31.
30) Kalita SJ, Bhardwaj A, Bhatt HA. Nanocrystalline calcium phosphate ceramics in biomedical engineering. Mater Sci Eng C Biomim Supramol Syst 2007; 27: 441-449.
31) Tran N, Webster TJ. Increased osteoblast functions in the presence of hydroxyapatite-coated iron oxide nanoparticles. Acta Biomater 2011; 7: 1298-1306.
32) Cerroni L, Filocamo R, Fabbri M, Piconi C, Caropreso S, Condò SG. Growth of osteoblast-like cells on porous hydroxyapatite ceramics: an in vitro study. Biomol Eng 2002; 19: 119-124.
33) Laranjeira MS, Fernandes MH, Monteiro FJ. Innovative macroporous granules of nanostructured-hydroxyapatite agglomerates: Bioactivity and osteoblast-like cell behaviour. J Biomed Mater Res A 2010; 95: 891-900.
34) Sato M, Aslani A, Sambito MA, Kalkhoran NM, Slamovich EB, Webster TJ. Nanocrystalline hydroxyapatite/titania coatings on titanium improves osteoblast adhesion. J Biomed Mater Res A 2008; 84: 265-272.
35) Chen L, Mccrate JM, Lee JCM, Li H. The role of surface charge on the uptake and biocompatibility of hydroxyapatite nanoparticles with osteoblast cells. Nanotechnol 2011; 22: 105708.
36) Okada S, Ito H, Nagai A, Komotori J, Imai H. Adhesion of osteoblast-like cells on nanostructured hydroxyapatite. Acta Biomater 2010; 6: 591-597.
37) Rogel MR, Qiu H, Ameer GA. The role of nanocomposites in bone regeneration. J Mater Chem 2008; 18: 4233-4241.
38) Shi Z, Huang X, Cai Y, Tang R, Yang D. Size effect of hydroxyapatite nanoparticles on proliferation and apoptosis of osteoblast-like cells. Acta Biomater 2009; 5: 338-345.
39) Samavini R, Sandaruwan C, De Silva M, Priyadarshana G, Kottegoda N, Karunaratne V. Effect of citric acid surface modification on solubility of hydroxyapatite nanoparticles. J Agric Food Chem 2018; 66: 3330-3337.
40) Moriguchi Y, Lee DS, Chijimatsu R, Thamina K, Masuda K, Itsuki D, *et al.* Impact of non-thermal plasma surface modification on porous calcium hydroxyapatite ceramics for bone regeneration. PLoS One 2018; 13: e0194303.
41) Shi X, Zhou K, Huang F, Wang C. Interaction of hydroxyapatite nanoparticles with endothelial cells: internalization and inhibition of angiogenesis in vitro through the PI3K/Akt pathway. Int J Nanomedicine 2017; 12: 5781-5795.
42) Lee WH, Zavgorodniy AV, Loo CY, Rohanizadeh R. Synthesis and characterization of hydroxyapatite with different crystallinity: effects on protein adsorption and release. J Biomed Mater Res A 2012; 100: 1539-1549.
43) Prabakaran K, Rajeswari S. Spectroscopic investigations on the synthesis of nano-hydroxyapatite from calcined eggshell by hydrothermal method using cationic surfactant as template. Spectrochim Acta A Mol Biomol Spectrosc 2009; 74: 1127-1134.
44) Stefanutti E, Papacci F, Sennato S, Bombelli C, Viola I, Bonincontro A, *et al.* Cationic liposomes formulated with DMPC and a gemini surfactant traverse the cell membrane without causing a significant bio-damage. Biochim Biophys Acta 2014; 1838: 2646-2655.
45) Cosimati R, Milardi GL, Bombelli C, Bonincontro A, Bordi F, Mancini G, *et al.* Interactions of DMPC and DMPC/gemini liposomes with the cell membrane investigated by electrorotation. Biochim Biophys Acta 2013; 1828: 352-356.
46) Saunders R, Szymczyk KH, Shapiro IM, Adams CS. Matrix regulation of skeletal cell apoptosis III: mechanism of ion pair-induced apoptosis. J Cell Biochem 2007; 100: 703-715.